JOURNAL OF AIRCRAFT
Vol. 46, No. 3, May–June 2009

Aerodynamics of Battle-Damaged Finite-Aspect-Ratio Wings

Peter M. Render,* Mujahid Samad-Suhaeb,† and Zhiyin Yang‡
Loughborough University, Loughborough, England LE11 3TU, United Kingdom
and
Mahmoud Mani§
Amirkabir University of Technology, 15875 Tehran, Iran

DOI: 10.2514/1.39839

Wind-tunnel tests have been carried out on a battle-damaged NACA 64_1–412 half-wing aspect ratio of 8.2. The simulated gunfire damage had a diameter of 0.2 wing chord and was located at midchord and at one of two spanwise locations. Tests were carried out at a Reynolds number of 5.5×10^5. Compared with an undamaged wing, the damage resulted in reduced lift, increased drag and a positive increase in pitching moment at zero lift. Moving the damage to near the tip reduced the magnitude of these effects. Using the static pressure difference between the upper and lower surfaces of the undamaged wing allowed the data from the present study to be successfully compared with previously published drag and lift data for a two-dimensional damaged airfoil. Tests on wings with aspect ratios of 6.2 and 10.3 produced similar trends in the aerodynamic characteristics and showed that the use of static pressure difference was equally effective in allowing comparisons with two-dimensional data.

Nomenclature

AR	=	aspect ratio
C_D	=	drag coefficient
C_L	=	lift coefficient
C_M	=	pitching-moment coefficient
C_P	=	static pressure coefficient
c	=	wing chord
dC_D	=	increment in drag coefficient due to damage
dC_{DA}	=	increment in drag area due to damage
dC_L	=	increment in lift coefficient due to damage
dC_{LA}	=	increment in lift area due to damage
dC_M	=	increment in pitching-moment coefficient due to damage
dC_{MA}	=	increment in pitching-moment area due to damage
dC_P	=	difference between upper- and lower-surface C_P
S	=	wing area
x	=	coordinate along the wing chord

Subscripts

damaged	=	results for a wing with simulated battle damage
undamaged	=	results for an undamaged wing

I. Introduction

RELATIVELY little research has been conducted into the aerodynamics of battle-damaged finite-aspect-ratio wings. Between 1967 and 1973, NASA Langley Research Center conducted tests on generic aircraft models in which the damage was simulated by removing all, or part, of the wings, tailplane, etc. The tests were conducted at high Mach numbers (1.41 to 4.63) and tended to concentrate on stability and control issues, although Hayes [1] and Spearman and Blair [2] did investigate general aerodynamic effects. In a second program, conducted on aircraft models with various percentages of the outer wing and tail removed, it was concluded that major damage may be sustained without causing the loss of the airplane or pilot [3]. This is an important conclusion because it indicates that a damaged aircraft will attempt to return to base. If the return is successful, the airplane will attempt to land, which indicates that low-speed characteristics, as well as those at cruise, are relevant in determining whether an aircraft will make a successful return.

The lack of low-speed data prompted the start of battle-damage studies at Loughborough University. Irwin [4] and Irwin and Render [5] conducted a series of wind-tunnel experiments in a low-turbulence wind tunnel to determine how the aerodynamic characteristics of a two-dimensional NACA 64_1–412 airfoil was influenced by the presence of simulated gunfire or missile damage. Using a wind-tunnel balance, the increments in the drag, lift, and pitching-moment coefficients, relative to an undamaged airfoil, were determined for each of the damage cases. To assist in the analysis, balance measurements were supplemented by flow visualization and surface static pressure readings.

The gunfire damage was represented by single circular holes with diameters ranging from 10 to 40% of airfoil chord c. The center of each hole was positioned at four different locations on the airfoil (i.e., leading edge, quarter-chord, half-chord, and trailing edge). It was concluded that increasing the hole diameter resulted in greater lift loss and increased drag and that the quarter- and half-chord locations produced the greatest adverse influence on aerodynamic performance. This influence on the aerodynamic coefficients was attributed to airflow through the hole. This flow was driven by the pressure differential between the upper and lower wing surfaces and took one of two forms. The first was a weak jet (Fig. 1) in which the flow through the hole formed an attached wake on the airfoil's surface. This gave relatively small changes in force and moment coefficients and resulted in a limited disruption of the pressure distribution on the surface of the wing. The second form (Fig. 2) resulted from either increased incidence or damage size. This was the strong jet in which the flow through the hole penetrated into the freestream, resulting in separation of the oncoming surface flow and the development of a separated wake with reverse flow. Compared with the weak jet, the effect on force and moment coefficients was increased, and the influence on the airfoil pressure distribution extended significantly in a spanwise direction.

Received 17 July 2008; revision received 18 December 2008; accepted for publication 14 February 2009.

*Senior Lecturer, Department of Aeronautical and Automotive Engineering. Senior Member AIAA.
†Research Student, Department of Aeronautical and Automotive Engineering.
‡Senior Lecturer, Department of Aeronautical and Automotive Engineering.
§Professor, Aerospace Engineering Department, Somaie Street, Hafez Avenue. Senior Member AIAA.

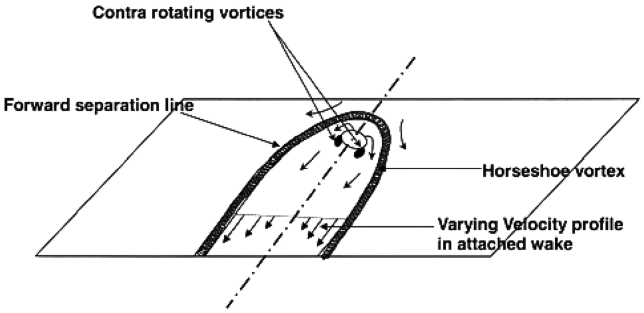

Fig. 1 Weak-jet flow characteristics.

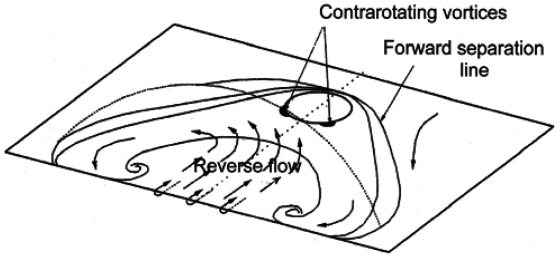

Fig. 2 Strong-jet flow characteristics.

II. Experimental Arrangement

The majority of tests were carried out on an untwisted constant-chord half-wing model with a nominal aspect ratio of 8 (AR8), supplemented with tests on models with nominal aspect ratios of 6 (AR6) and 10 (AR10). All of the models were tested in the Loughborough University 1.9×1.3 m closed-working-section wind tunnel. The airfoil section was a NACA 64_1–412. The wings were manufactured from the molds used to produce the models for Irwin's [4] two-dimensional studies and, consequently, the airfoil sections were identical. Structural considerations in the design of the wind-tunnel model dictated a wing of solid cross section reinforced by two steel rods running along the span of the model. There was no attempt to model the typical internal structure of an aircraft wing. Each model was constructed from interchangeable panels, which allowed one battle-damaged panel to be manufactured and then positioned at different spanwise locations, as shown in Table 1. Note that for each model, the furthest outboard damage was located at 162 mm from the tip. The models were originally tested with an additional damage location at 150 mm from the wing root. Analysis of the data indicated that the presence of the wind-tunnel floor at the wing root was influencing the development of the flow through the damage, and the decision was made to omit these data.

As previously indicated, Irwin [4] showed that for simulated gunfire damage, the greatest effects occurred for damage located at quarter- and half-chord. The presence of the two reinforcing steel rods in the model meant that the only practical location for the damage was at half-chord. In addition, the diameters and locations of the rods dictated that a circular hole of 20% chord diameter was the largest of Irwin's simulated-gunfire-damage cases that could be accommodated. In summary, this paper investigates the influence of simulated gunfire damage by testing a single hole of 20% chord diameter located at midchord and at different spanwise locations. Render et al. [6] and Mani and Render [7] showed that the use of circular holes to simulate gunfire is an acceptable technique and produces similar results to more representative damage shapes.

To determine lift, drag, and pitching-moment effects, the half-models were mounted on an underfloor six-component balance. Prior calibration of the balance indicated that nominal accuracy for the AR8 wing would be better than $C_L = 0.0003$, $C_D = 0.0001$, and $C_M = 0.0002$. Uncertainty and repeatability for both the damaged and undamaged AR8 wings were determined to be $C_L = \pm 0.005$, $C_D = \pm 0.0003$, and $C_M = \pm 0.0005$. Wind-tunnel corrections were determined by applying the methods of Maskell, as described by Barlow et al. [8], and Krynytzky [9]. Before investigating damage effects, the wings were tested in their undamaged states. In addition to providing datum cases against which the damage tests could be compared, the undamaged tests allowed the authors to determine that the models were performing as expected. Tests were run at a wind speed of 40 m/s, giving a nominal Reynolds number of 5.5×10^5. Turbulence intensity at these conditions was less than 0.15%.

Because of the construction of the model, the number of static pressure tappings that could be installed was limited. A pressure-tapped undamaged wing panel was produced with sufficient upper-surface tappings installed to allow the general shape of the measured profile to be assessed for realism, and so instill a degree of confidence in the pressure measurements. When the pressure-tapped panel was installed, the tappings were located at the same spanwise locations used for the damage. A single tapping was also provided on the lower surface at 50% chord, which corresponded to the center of the damage hole. Static pressure measurements were carried out using a 48D9 Scanivalve with a Furness FCO44 pressure transducer of nominal accuracy of ±0.2% of reading. The general repeatability of the pressure measurements were typically $C_P = \pm 0.003$.

Balance and pressure measurements were supplemented with surface flow visualization using a mixture of titanium dioxide, linseed oil, and paraffin. Interpretation of the flow visualization allowed key features of the damage flows to be identified and, in particular, allowed classification of the damage jets. The adopted classifications were developed from Irwin's [4] criteria: namely,

1) A weak jet is identified by an attached wake behind the damage hole and a clearly defined horseshoe vortex.

2) A strong jet is indicated by a pair of vortices, located on the airfoil's surface behind the damage, which induced reverse flow from the trailing edge.

3) For a transitional jet, the transition from weak to strong jet is not necessarily instantaneous, and the resulting flow visualization can appear to be neither a weak or strong jet. The presence of the transitional jet was verified by carrying out further flow visualization at lower incidences (typically 1 deg less) to confirm the presence of the weak jet and at higher incidences (typically 1 deg more) to confirm the presence of the strong jet.

III. Experimental Results

In their undamaged states, all three wings compared favorably with predicted three-dimensional results, which were determined from the two-dimensional data for the NACA 64_1–412 generated by Irwin [4]. These tests confirmed that all three wings were operating close to their nominal aspect ratios. For example, the AR8 model had a lift-curve slope of 0.0818/deg, compared with a predicted value of 0.0843/deg. The discrepancy was attributed to the boundary layer on the tunnel floor and to the small gap between the model and the tunnel floor. This gap was required to allow balance measurements to be made.

Table 1 Model geometries

Model name	AR6	AR8	AR10
Chord	197 mm	197 mm	197 mm
Span	612 mm	812 mm	1012 mm
True aspect ratio	6.21	8.24	10.27
Damage locations (from wing root)	450 mm	450, 650 mm	450, 650, 850 mm

The influence of the battle damage was determined by comparing the results for the damaged wings with those of the corresponding undamaged wings. This allowed the following coefficient increments to be defined:

$$dC_L = C_{L\text{damaged}} - C_{L\text{undamaged}} \quad (1)$$

$$dC_D = C_{D\text{damaged}} - C_{D\text{undamaged}} \quad (2)$$

$$dC_M = C_{M\text{damaged}} - C_{M\text{undamaged}} \quad (3)$$

For each damage case, the aerodynamic coefficient data was the average of three separate wind-tunnel runs, whereas the undamaged data came from an average of five runs. The results of the AR8 wing will be discussed in detail and, when appropriate, these will be supplemented with data for the other aspect ratios.

A. Flow Visualization of the AR8 Wing

Flow-visualization photographs for the damage located at 450 mm are shown in Fig. 3. These photographs show the upper-surface flows at incidences of 4 and 8 deg. The flow direction for these and subsequent photographs is from top to bottom, with the outboard side of the wing on the left. At the lower incidence, the most prominent feature is the laminar separation bubble, which is a characteristic of the airfoil section at relatively low Reynolds numbers (denoted as A). At the damage, the laminar separation bubble is distorted so that the laminar separation occurs ahead of the hole. Meanwhile, there is a jet issuing from the damage hole. The presence of the jet is indicated by the following:

1) A pair of contrarotating vortices is immediately behind the damage hole (B).

2) Flow lines on either side of the hole emerge from the hole between the laminar separation bubble and the contrarotating vortex pair (C).

3) A horseshoe vortex is on the outboard side of the damage (D). At the corresponding inboard position, there is a faint white line, which suggests a much weaker horseshoe vortex.

The presence of the horseshoe vortex indicates the existence of a weak jet, but the lack of a strong horseshoe vortex on the inboard side suggests that the damage jet is undergoing transition to a strong jet.

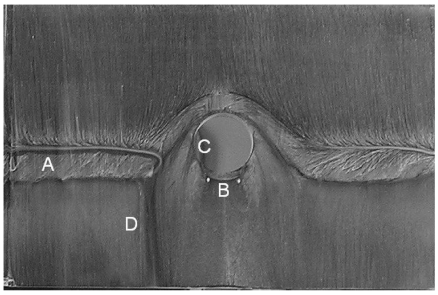

a) 4 deg incidence

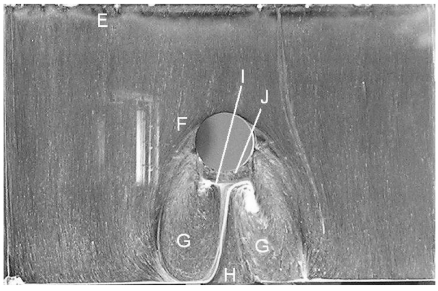

b) 8 deg incidence

Fig. 3 Circular 20%c damage at 450 mm from the root of the AR8 wing; (flow direction is from top to bottom; outboard side is on the left).

There was concern that the presence of the laminar separation bubble was responsible for the asymmetry. This possible influence was investigated by forcing boundary-layer transition forward of the damage. Flow visualization indicated that the damage jet was still transitional and asymmetric between the inboard and outboard sides. The only effect of the laminar separation bubble was to delay the onset of transitional conditions in the damage jet. Careful inspection of the damaged wing panel failed to identify any asymmetry in its geometry that was likely to cause the observed flow patterns. Finally, the possible influence of gravity from mounting the model vertically was discounted, because tests carried out in an open-jet wind tunnel with a horizontally mounted AR6 wing with simulated battle damage produced similar asymmetric flow patterns.

Confirmation of the asymmetric nature of damage flow was provided by another study that used star-shaped damage. The study used the present AR8 wing, but used a completely new damaged wing panel. The panel had previously been tested as a two-dimensional wing and the flow through the damage was symmetric. However, as shown in Fig. 4, when the damage was placed in the AR8 wing, it was asymmetric. The flow through the star is more complicated than for a circle, but the horseshoe vortex on the outboard side can be identified, whereas it is not present on the inboard side. The flow is behaving as a weak jet on the outboard side and is transitional on the inboard side. Render et al. [6] and Mani and Render [7] provided a detailed description of the flow through star-shaped damage, and these references can be consulted to help interpret the flow regimes in Fig. 4.

For the AR8 wing, it was therefore concluded that the asymmetry observed in the damage jet was a genuine effect and was possibly caused by the spanwise variation of static pressure associated with finite-aspect-ratio wings. Because of the limited number of static pressure tappings on the model, it was not possible to measure the spanwise pressure variation experimentally. However, Samad-Suhaeb [10] used the commercial computational fluid dynamics software FLUENT to investigate the theoretical aerodynamic characteristics of the AR8 wing in both its damaged and undamaged states. For the undamaged case, the numerical model consisted of a grid of 395 000 cells. The Spalart–Allmaras turbulence model was used, because its use in studies on two-dimensional battle-damaged airfoils had previously produced reasonable results [10]. Figure 5a shows the theoretical pressure coefficient C_P distributions for the undamaged wing at 4 deg of incidence. Two locations are shown: one is 60 mm inboard of the center of the hole location on the damaged wing (i.e., at 390 mm from the wing root) and the other is 60 mm outboard of the center (i.e., at 510 mm from the root). On the damaged wing, these locations would correspond to 1.5 times the hole diameter inboard and outboard. The pressure distributions at the two locations are similar, but not identical. Close inspection reveals that at $x/c = 0.5$ (i.e., the center of the hole on the damaged wing), moving outboard results in a small reduction in the upper-surface C_P of 0.01. At the same x/c, the difference between the upper- and lower-surface C_P reduces by 0.02 while moving outboard. These small differences may be associated with the

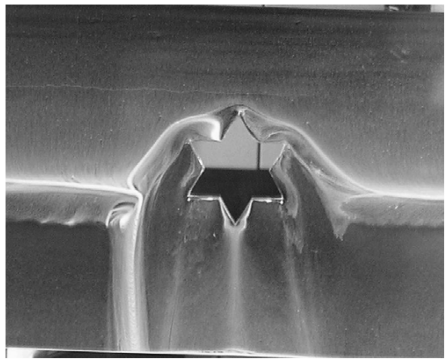

Fig. 4 Star-shaped damage at 450 mm from the root of the AR8 wing with an incidence of 4 deg (flow direction is from top to bottom; outboard side is on the left).

observed flow asymmetry in the damage jet. The theoretical studies of Samad-Suhaeb [10] did, in fact, show asymmetry in the damage flow at 4 deg of incidence, which adds further support to the suggestion that small pressure differences can result in flow asymmetry.

Figure 5b shows the C_P distributions at the two locations for 8 deg of incidence. Compared with 4 deg, the difference between the upper- and lower-surface C_P has increased at both locations. At $x/c = 0.5$, moving outboard results in a small reduction in the upper-surface C_P of 0.02. At the same x/c, the difference between the upper- and lower-surface C_P reduces by 0.03 while moving outboard. Based on Fig. 5b, it would be anticipated that the damage jet would be stronger than at 4 deg, but would still be asymmetric.

Returning to the flow visualization, increasing incidence to 8 deg did increase the strength of the damage jet so that it displayed the characteristics of a strong jet (Fig. 3b). In this figure, the laminar separation bubble (E) is now located close to the wing's leading edge, and the flow on the airfoil's surface (i.e., approaching the damage) is turbulent. At the leading edge of the hole, the airfoil surface flow encounters the damage jet and is deflected around the damage (F). It is then entrained into the large vortex pair positioned behind the damage on the airfoil's surface (G). Between the two vortices of the vortex pair is a triangular region of reverse flow (H), which moves toward the damage hole before separating from the surface, as indicated by the line of white flow-visualization liquid (I). Immediately behind the hole, there is a small region in which the damage jet has expanded on exit from the hole (J), and the air flows downstream before appearing to separate from the airfoil's surface at the same position as the reverse flow (I). This separation position is the downstream edge of the damage jet and suggests that the previously mentioned reverse flow is entrained into the damage jet.

The damage jet is still asymmetric at 8 deg. This is particularly evident on the entrained flow into the large vortices behind the damage, which is more prominent on the outboard side. It should also be noted that the spanwise extent of the wake behind the damage is larger for the strong jet than for the weak jet and would suggest a greater adverse impact on the aerodynamic performance of the wing.

Moving the damage out toward the wing tip resulted in increased asymmetry in the damage flow (Fig. 6). In this figure, the tip is on the left-hand edge of the photographs. The white vertical line to the right of the tip is the joint line between the damaged wing panel and the tip

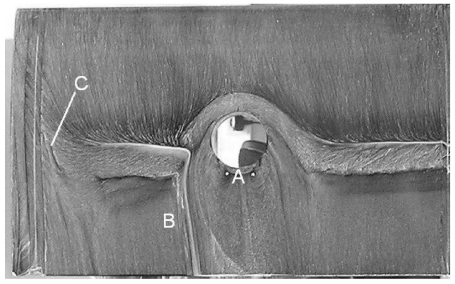

a) 4 deg incidence

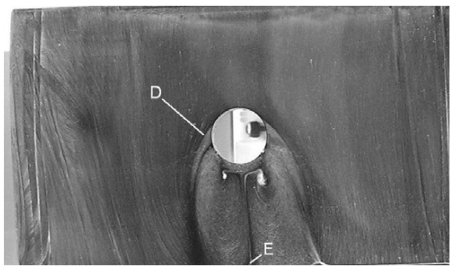

b) 8 deg incidence

Fig. 6 Circular 20%c damage near the tip of the AR8 wing (650 mm from the root); (flow direction is from top to bottom; outboard side is on the left).

and has no bearing on the flow visualization, other than confirming that the joint did not adversely affect the flow. The theoretical C_P distributions near the tip of the undamaged AR8 wing are shown in Fig. 7. These were obtained by Samad-Suhaeb [10] using FLUENT. Once again, two locations 60 mm from either side of the damage center location are shown The inboard location is 590 mm from the wing root and the outboard location is 710 mm. Comparing the distributions for 4 deg (Fig. 7a) and 8 deg (Fig. 7b) with the midspan results (Fig. 5) shows that around the region to be occupied by the damage ($x/c = 0.5$), the magnitudes of the upper- and lower-surface C_P are reduced and, as a consequence, so is the static pressure

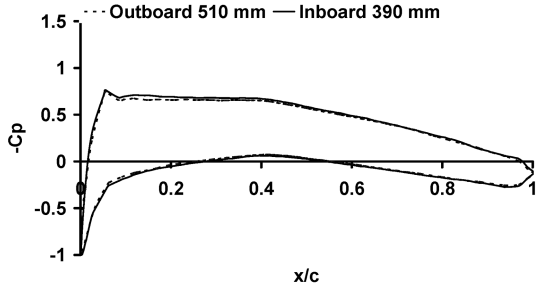

a) 4 deg incidence

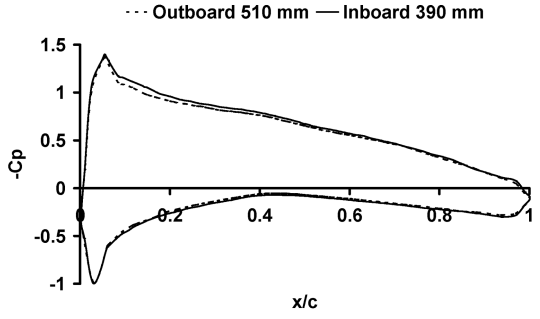

b) 8 deg incidence

Fig. 5 Theoretical pressure coefficient distributions near the mid-damage location for an undamaged AR8 wing.

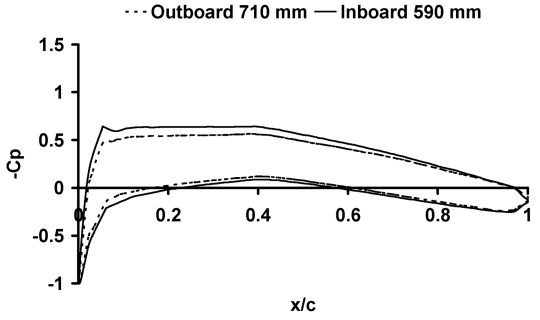

a) 4 deg incidence

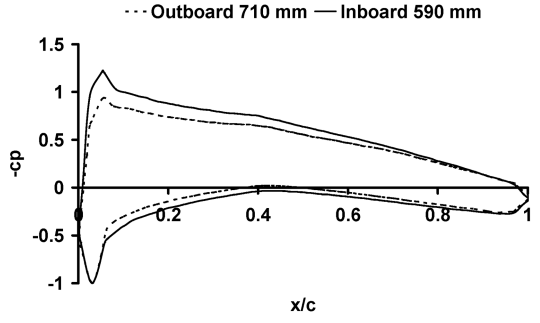

b) 8 deg incidence

Fig. 7 Theoretical pressure coefficient distributions near the tip damage location for an undamaged AR8 wing.

difference between the two surfaces. It is also apparent that the differences between the inboard and outboard stations are more significant in Fig. 7. Based on these observations, it is probably reasonable to expect that the damage jet would be weaker near the tip, but more asymmetric than at midspan.

For 4 deg incidence, close inspection of Fig. 6a reveals that the pair of contrarotating vortices (A) are slightly closer together than for the midspan case (Fig. 3a), which indicates that the damage jet is slightly weaker. There is also asymmetry in the flow, because the horseshoe vortex that is apparent on the outboard side is inclined inboard (B). This inclination may be due in part to the trailing vortex from the tip of the wing, which is in the early stages of development. The trailing vortex itself can be seen on the left-hand edge of the photograph as inclined streaklines, and its destruction of the laminar separation bubble is particularly apparent (C). The increased asymmetry is also apparent at 8 deg (Fig. 6b). Compared with the midspan location (Fig. 3b), the following observations can be made for 8 deg incidence:

1) At the tip, the damage jet is running less full; that is, the forward separation line is slightly behind the leading edge of the hole (D).

2) The extent of the reverse flow between the large vortices is much reduced at the tip (E). This indicates that near the tip, the damage jet has not yet fully developed into a strong jet and may be regarded as transitional.

3) Near the tip, the spanwise extent of the damage wake is reduced.

All of these observations are consistent with the reduced effective incidence that would be present near the tip and with the resulting reduced pressure difference between the upper and lower wing surfaces.

At both damage locations, increasing incidence above 8 deg resulted in the damage jet getting stronger, as was evident from the increased spanwise extent of the wake behind the damage. However, at both locations, the jet still retained its asymmetry.

B. Aerodynamic Coefficient Increments of the AR8 Wing

The coefficient increments are shown in Fig. 8 for both damage locations. As expected, damage reduces the lift and increases the drag coefficients of the wing. Because of the increasing strength of the damage jet, the magnitudes of these effects increase with incidence. Moving the damage toward the tip (650 mm) reduces the lift and drag increments when compared with the 450 mm damage location. These trends are consistent with the previously described weakening of the damage jet at the tip location. Around the zero-lift incidence of −2.7 deg, there was little flow through the damage and the hole effectively acted as a cavity. This results in small residual lift and drag-coefficient increments at negative incidences and a decrease in the pitching-moment coefficient. Increasing incidence make the pitching-moment coefficient increments more negative (i.e., nose down). Irwin [4] showed that the pressure in the wake was reduced downstream of battle damage and that these effects increased with incidence. Such an effect would result in a nose-down pitching moment and is consistent with the trends shown in Fig. 8c. The pitching-moment effects are diminished as the damage is moved toward the tip and this is again consistent with a weakening of the damage jet.

Also shown in Fig. 8 are the increments based on Irwin's [4] two-dimensional results, which are denoted as 2-D Irwin [4]. Irwin reduced his data to coefficient form using the planform area of the wing. Therefore, his values of dC_L, dC_D, and dC_M have been converted to the three-dimensional case by multiplying with the area ratio (i.e., two-dimensional wing area divided by three-dimensional wing area). Because the model chords are identical, this reduces simply to the ratio of the wing spans. Irwin's [4] two-dimensional data were collected at a lower Reynolds number of 5×10^5. However, tests were carried out during the present study and showed that there was no measurable change in the increments between Reynolds numbers of 5×10^5 and 6×10^5. From Fig. 8 it is clear that although Irwin's data show the right trends with incidence, the size of the increments are overestimated. There will be a slight mismatch between the incidences, because Irwin's values are two-dimensional,

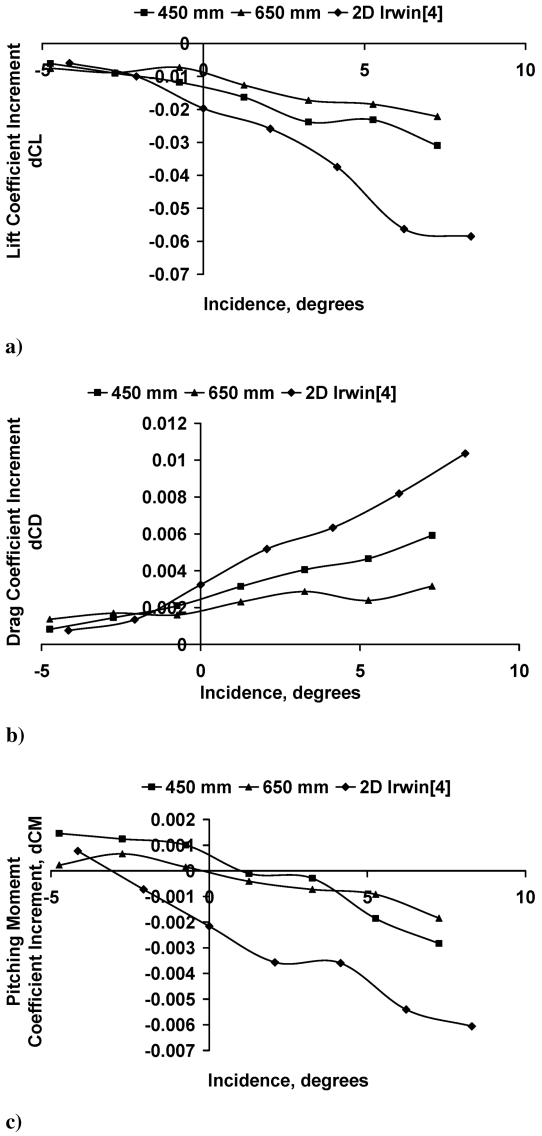

Fig. 8 Variation of lift, drag, and pitching-moment coefficient increments with incidence; 20%c damage at 450 and 650 mm from the root of the AR8 wing.

whereas the present study uses nominal model incidence that has not been corrected for the spanwise variation induced by tip effects. However, this omission will not account for the differences.

Figure 9 shows the flow visualization for the two-dimensional airfoil used by Irwin [4], and it is immediately clear that a strong jet exists at both incidences. This can be compared with the present study (e.g., Fig. 3), in which a weak jet existed at 4 deg incidence and a strong jet exists at 8 deg. Irwin showed that a strong jet will produced greater coefficient increments than a weak jet, and so this is likely to account for some of the difference at 4 deg. Comparing the 8 deg cases, the two-dimensional strong jet has a more extensive impact on the wing flow than the three-dimensional case. This indicates that the damage jet for the two-dimensional wing is significantly stronger and will result in significantly larger coefficient increments. It is also instructive to compare the jet at 4 deg for the two-dimensional wing with 8 deg of the three-dimensional wing. The wakes behind the holes are similar in spanwise extent, although the region of reverse flow between the two large vortices is more prominent for the two-dimensional case. This suggests that the two-dimensional case has a stronger jet and would explain why, even at low incidences, the data from Irwin produce larger increments than were seen at the highest three-dimensional incidences.

The static pressure difference between the upper and lower wing surfaces is thought to determine the characteristics of the damage jet.

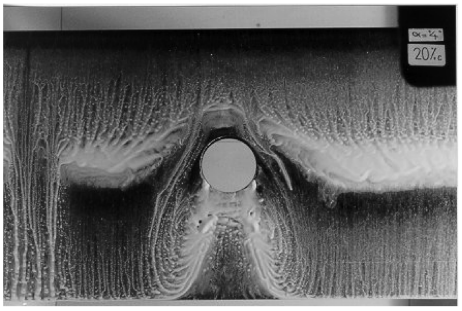

a) 4 deg incidence

b) 8 deg incidence

Fig. 9 Circular 20%c damage located at midchord of the two-dimensional airfoil (flow direction is from top to bottom).

Although the pressure field in the vicinity of damage is likely to be complicated, it may be possible to use static pressure characteristics of an undamaged wing to convert two-dimensional damage data to three dimensions. As already indicated, construction of the model meant that only one tapping could be provided on the lower surface, at 50% chord, which corresponded to the damage center. As previously described, theoretical predictions of the pressure distributions around the undamaged AR8 wing were carried out by Samad-Suhaeb [10] using the FLUENT software package. These predictions included the distributions shown in Figs. 5 and 7. From these figures, it can be seen that for all plots, from $x/c = 0.4$ to 0.6, the mean C_P difference between the upper and lower surfaces is close to the value at $x/c = 0.5$. This proved to be true over the considered incidence range of -5 to 10 deg and led to the conclusion that using the C_P difference at 50% chord was close to the mean of the C_P difference over the area that would be occupied by the relatively small damage hole. Although more lower-surface pressure tappings would have been desirable, it was concluded that the availability of the C_P difference at the location of the damage center was sufficient to investigate the potential of data analysis techniques.

For the undamaged-wing experiments, differencing the readings of the upper- and lower-surface pressure tappings at 50% chord allowed a differential pressure coefficient dC_P to be calculated. This was done for both the 650 and 450 mm damage locations. The corresponding two-dimensional pressure measurements are available from Irwin [4]. Figure 10 shows the coefficient increments plotted against dC_P. Particularly for the lift and drag increments, the two-dimensional results from Irwin are closer to the finite-aspect-ratio wing values, although they still overestimate the three-dimensional results. An interesting side effect of plotting against dC_P is that, for both dC_L and dC_D, the two damage locations on the finite-aspect-ratio wing are closer together. For both increments, the difference between the results for the two damage locations is generally comparable with the previously noted repeatability for C_L and C_D. The main exception occurs for dC_D, in which the results for the two damage locations diverge when dC_P is greater than 0.5. The 650 mm location was only 162 mm from the wing tip and, as discussed later, the proximity of the tip is believed to be significant.

For dC_M, plotting against dC_P is not so successful in bringing the results for the two damage locations closer together, with both

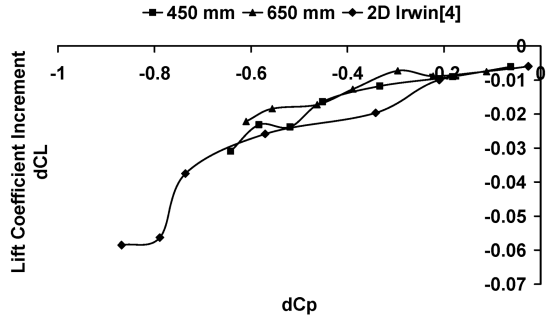

a)

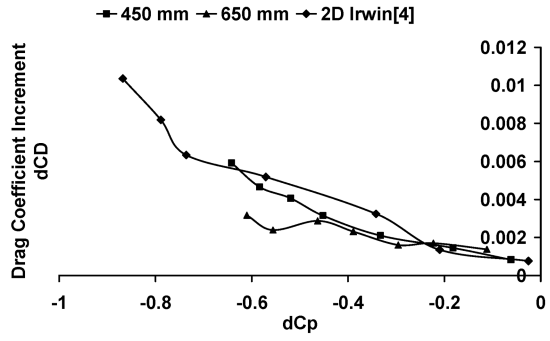

b)

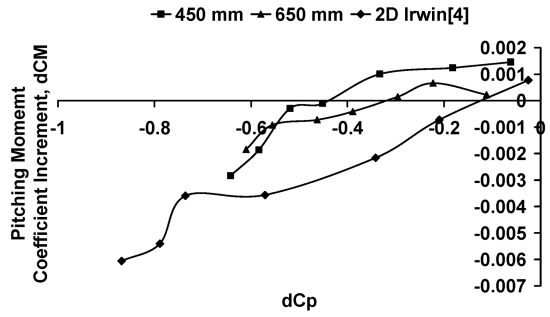

c)

Fig. 10 Variation of lift, drag, and pitching-moment coefficient increments with differential pressure coefficient; 20%c damage at 450 and 650 mm from the root of the AR8 wing.

locations also significantly offset from the results based on Irwin's [4] two-dimensional data. Recalling the asymmetry of the damage flowfields and noting the relatively large distance behind the moment reference center at quarter-chord, it is likely that any small changes in surface pressures behind the damage may have a significant influence on pitching moment. Given this and the crude method of calculating dC_P, the use of dC_P in its present form is unlikely to be successful.

These results for dC_L and dC_D suggest that the effects of damage at one location of a finite-aspect-ratio wing can be used to predict the effect of damage at another location if static pressure measurements for an undamaged wing are available. It is recognized that using the value of dC_P at a single point will always produce an approximate estimate of battle-damage effects. These approximations are likely to become more unacceptable as the damage size increases. However, it is likely that integrating the pressure difference across all of the damage hole area will produce better results. Unfortunately, due to limitations in the construction of the model, it has not been possible to investigate further refinements to the technique. However, the applicability of the technique to other aspect ratios can be investigated.

C. AR6 and AR10 Wings

The AR6 and AR10 wings exhibited the same general trends in damage flow and coefficient increments that have already been

identified for the AR8 wing. For reasons of succinctness, these trends are not discussed here, but a comprehensive discussion is given by Samad-Suhaeb [10]. Instead, the AR6 and AR10 wings will be used to further assess the usefulness of the differential pressure coefficient. A comparison of all three aspect ratios is shown in Fig. 11 for the damage located 450 mm from the wing root. For this comparison, the increments are in terms of incremental lift, drag, and pitching-moment areas, defined as

$$dC_{\mathrm{LA}} = dC_L \cdot S \tag{4}$$

$$dC_{\mathrm{DA}} = dC_D \cdot S \tag{5}$$

$$dC_{\mathrm{MA}} = dC_M \cdot S \tag{6}$$

where dC_L, dC_D, and dC_M are the previously defined coefficient increments, and S is the wing area. Note that the chord has not been included in the definition of dC_{MA}, because all of the models had the same chord. The use of lift, drag, and pitching-moment area increments removes the dependency of coefficient increments on wing area and so ensures that distortions due to wing size do not influence comparisons between the three damaged wings. This approach is entirely consistent with aircraft drag analysis, in which drag area is frequently used instead of drag coefficient.

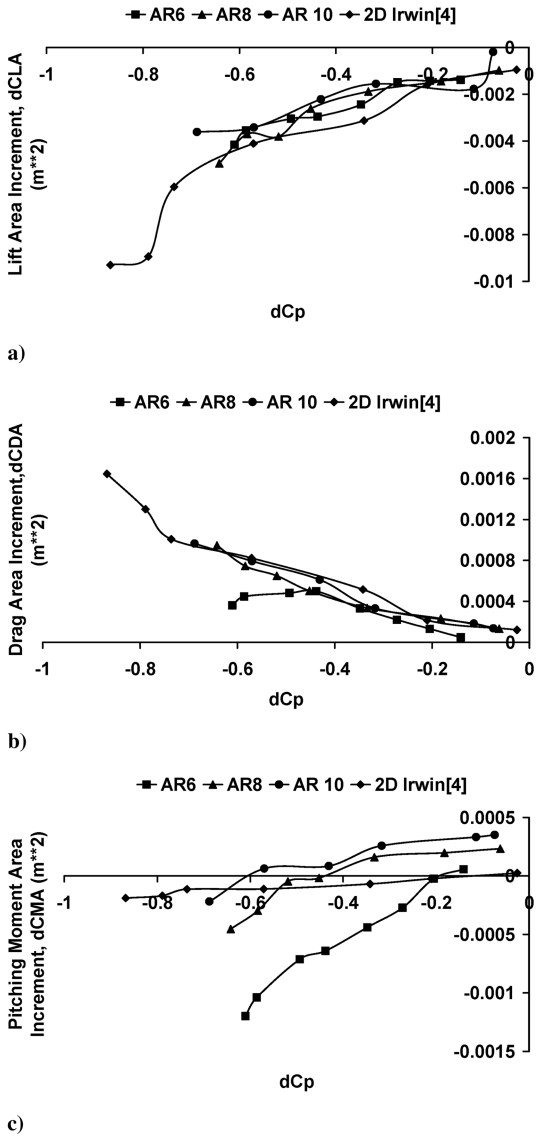

Fig. 11 Lift, drag, and pitching-moment area increments against differential pressure coefficient; 20%c damage at 450 mm from the root for all wings.

The lift area increments are shown plotted against differential pressure coefficient in Fig. 11a; away from the extreme ends of the curves, the three aspect ratios typically lie within a band of 0.001 m^2. This is consistent with the previously noted repeatability for C_L of ± 0.005, which can be expressed as a lift area of ± 0.0008 m^2 for the AR8 wing. This potential scatter in the data means that it is difficult to discuss the plotted curves in any great detail, but plotting the data against differential pressure coefficient has essentially removed dependence on aspect ratio. Comparing the three aspect ratios with the lift area increment derived from Irwin's [4] two-dimensional data indicates that the data from the present study are generally lower. However, it would appear that two-dimensional data could be used to make a reasonable assessment of likely three-dimensional effects. The extreme ends of the curve for the AR10 wing appear to be out of alignment with the other two aspect ratios. The lowest dC_P correspond to low-lift conditions when increments are determined by subtracting two small values from each other, and repeatability issues can become significant. Close inspection of the data showed that all of the runs used to produce the data were inside the noted repeatability. With no obvious errors, all of the data have been retained, especially because drag data appeared to be consistent. Similarly, the data for the AR10 wing at the highest dC_P were within repeatability limits and have been retained.

The drag area increments are shown in Fig. 11b. Based on the previously noted C_D repeatability, the drag area repeatability is ± 0.00005 m^2. This suggests that the AR10 and AR8 results can be considered well aligned and close to Irwin's [4] two-dimensional data. The most notable feature of Fig. 11b is the behavior of the AR6 case, which diverges from the other two aspect ratios. The damage hole on the AR6 is only 162 mm from the tip and, as shown in Fig. 6, the close proximity of the trailing vortex may lead to some modification of the damage jet flow and increase its asymmetry. The divergence of the curve coincides with the onset of strong-jet conditions. What is surprising is that the drag increment stays roughly constant, because strong jets are associated with rapid increases in drag. A similar trend was also shown for the AR8 wing, with the damage located 162 mm from the tip (i.e., damage located at 650 mm from the wing root), as shown in Fig. 12. Both the AR6 and AR8 curves lie below Irwin's two-dimensional data and level out around $dC_P = 0.5$. For AR8, this is also the onset of strong-jet conditions. Detailed investigation of the possible flow interaction between the tip vortex and the damage jet has not been carried out, but it is thought likely that the presence of the vortex may suppress the development of the separated wake of the strong jet.

The pitching-moment area increments are shown in Fig. 11c. The slope of the AR6 data is shallower than the other two aspect ratios and Irwin's [4] two-dimensional results. The previously suggested interaction between the tip vortex and the damage jet may possibly account for the results. Based on the previously noted repeatability for the AR8 model, the repeatability of the dC_{MA} data is typically ± 0.00008 m^2. This is similar to the difference in the AR10 and AR8 results, particularly at low dC_P. At higher dC_P, the gradient of the curves for these two aspect ratios increases and starts to diverge from Irwin's two-dimensional data. This occurs at the onset of strong-jet conditions and suggests that for pitching moment, the use of dC_P

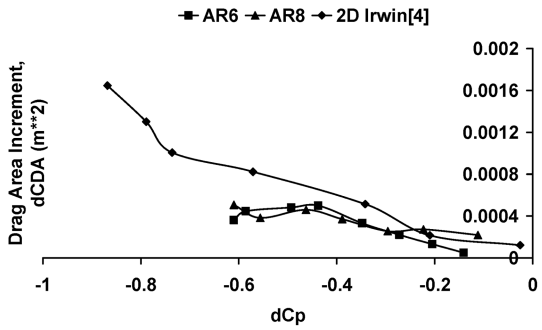

Fig. 12 Drag area increments for AR6 and AR8 wings; 20%c damage at 162 mm from the tip.

from a single point is questionable in the highly-three-dimensional flow of the strong jet.

IV. Conclusions

1) On finite-aspect-ratio wings, flows through simulated gunfire damage are asymmetric; that is, differences exist when comparing inboard and outboard sides of the damage. This asymmetry is possibly driven by the spanwise variation of static pressure associated with finite-aspect-ratio wings, although this needs to be verified by further investigation.

2) Adding damage resulted in a lift-coefficient decrement that increased in magnitude with incidence. Moving the damage toward the tip reduced the magnitude of these effects.

3) Adding damage resulted in a drag-coefficient increment that increased with incidence. Moving the damage toward the tip reduced the magnitude of these effects.

4) At the zero-lift incidence, the damage produced a positive increase in pitching-moment coefficient. Increasing incidence resulted in a more negative pitching-moment coefficient. Moving the damage to the tip reduced the magnitude of the initial increment and the incidence effects.

5) At a damage location on a finite-aspect-ratio wing, the static pressure difference between the upper and lower surfaces of the undamaged wing can be used to predict the likely effects of damage on drag and lift coefficients. This can be done by using data from either a damaged two-dimensional airfoil or a different damage location on the finite-aspect-ratio wing. The application of this method to pitching-moment coefficients proved to be of limited success.

Acknowledgments

The authors are grateful for the help and assistance of Peter Stinchcombe and Rob Hunter in manufacturing the models. The help of Pat Griffin in producing some of the figures is also gratefully acknowledged. Thanks are also extended to Andrew Irwin, who provided the two-dimensional midchord damage photographs.

References

[1] Hayes, C., "Effects of Simulated Wing Damage on the Aerodynamic Characteristics of a Swept Wing Airplane Model," NASA TMX-1550, Apr. 1968.

[2] Spearman, M. L., and Blair, A. B., "Wind Tunnel Studies of Simulated Damage to Aerodynamic Surfaces of Airplanes," NASA TMX-2550, Apr. 1972.

[3] Spearman, M. L., "Wind Tunnel Studies on the Effects of Simulated Damage on the Aerodynamic Characteristics of Airplanes and Missiles," NASA TM-84588, Dec. 1982.

[4] Irwin, A. J., "Investigation into the Aerodynamic Effects of Simulated Battle Damage to a Wing," Ph.D. Thesis, Loughborough Univ., Loughborough, England, U.K., May 1999.

[5] Irwin, A. J., and Render, P. M., "The Influence of Mid-Chord Battle Damage on the Aerodynamic Characteristics of Two-Dimensional Wings," *The Aeronautical Journal*, Vol. 104, No. 1033, 2000, pp. 153–161.

[6] Render, P. M., de Silva, S., Walton, A. J., and Mahmoud, M., "Experimental Investigation into the Aerodynamics of Battle Damaged Airfoils," *Journal of Aircraft*, Vol. 44, No. 2, 2007, pp. 539–549. doi:10.2514/1.24144

[7] Mani, M., and Render, P. M., "Experimental Investigation into the Aerodynamic Effects of Airfoils with Triangular and Star-Shaped Through Damage," AIAA Paper 2005-4978, June 2005.

[8] Barlow, J. B., Rae, W. H., and Pope, A., "Boundary Corrections 2: Three Dimensional Flow," *Low Speed Wind Tunnel Testing*, 3rd ed., Wiley, New York, 1999, pp. 367–427.

[9] Krynytzky, A., "3D Lift Interference for a wings of Finite Span," *Wind Tunnel Wall Corrections*, AGARD Rept. AG-336, Neuilly-sur-Seine, France, Oct. 1998, pp. 2.14–2.22.

[10] Samad-Suhaeb, M., "Aerodynamics of Battle Damaged Finite Aspect Ratio Wings," Ph.D. Thesis, Loughborough Univ., Loughborough, England, U.K., Apr. 2008.